



Influence of Design Elements on the Induced-EMF and Flux Linkage of Double Stator Permanent Magnet Machine

C. C. Awah*, O. I. Okoro, G. C. Diyoke, A. J. Onah

Department of Electrical and Electronic Engineering, Michael Okpara University of Agriculture, Umudike, Nigeria
*awahchukwuemeka@gmail.com

Research Article

Abstract

The influence of design elements such as conductor space opening / stator-tooth pitch proportion (β), permanent magnet width (PM_w), rotor circular width (R_{rh}), aspect ratio (S_r), stator tooth-width (T_w), outer rotor pole arc / pitch proportion (Y_1) and inner rotor pole arc / pitch proportion (Y_2), on open circuit machine performances such as flux linkage and induced electromotive force (EMF) is investigated in this study using finite element method. The studies show that for each machine element, there is a point or dimensional position upon which the largest machine output performance is realized. Moreover, smooth control of any given electrical machine would also depend on these structural elements. The largest induced electromotive force is obtained when the conductor space / rotor pitch proportion, permanent magnet width, rotor circular width, aspect ratio, stator tooth-width, and outer and inner rotor pole arcs / pitch proportion is: 0.7, 5mm, 5mm, 0.7, 6mm, 0.7 and 0.3, respectively. Corresponding largest flux linkage amplitudes also occur at these geometric values, owing to the direct relationship between electromotive force and flux linkage. The analyzed machine would be most appropriate for direct-drive operations.

Copyright © Faculty of Engineering, Ahmadu Bello University, Zaria, Nigeria.

Keywords

Design elements; Electromotive force; Flux linkage; Twin stator

Article History

Received: – October, 2021

Accepted: – April, 2022

Reviewed: – January, 2022

Published: – April, 2022

1. Introduction

Over time, research has shown that geometric design elements are key factors in determining the output performance of any given electrical machine, as evidenced in (Thomas *et al.*, 2009) and (Zhang *et al.*, 2017). Thus, a comprehensive study on the influence of design elements on induced-electromotive force and phase flux linkage of a double stator permanent magnet machine is presented in this current study.

A time-saving analytical finite element approach of predicting machine performance using mathematical model equations is proposed and presented in (Lekic and Vukosavic, 2020). However, the developed analytical method may be associated with lower result accuracy compared to the obtainable finite element analysis results, despite the additional advantage of the model's improved fault-tolerant ability. This precision drawback is inherent in most analytical methods, owing to its attendant numerous assumptions. Also, the impact of split ratio on torque-density of flux-switching permanent magnet machine (FSPM) is presented in (Li *et al.*, 2012). The studies show that effect of split ratio on torque-density of flux-switching permanent magnet machines is more prominent than that obtained in other traditional PM machines of similar size, owing to the sandwiched nature of its permanent magnets (PMs) on the stator section of FSPM machines. The studies further revealed through analytical technique, that there is a direct proportionality between the split ratio and the overall machine radius of a flux-switching PM machine.

Similarly, it is demonstrated in (Li *et al.*, 2011) that the electromagnetic performance of an electric machine could be greatly enhanced by suitable optimization and selection of the most appropriate geometric dimension such as, magnet size, radial width of the pole-piece, back-iron, etc. More so, optimization of rotor pole arc ratio of dual stator permanent magnet machine is given in (Wei and Nakamura, 2020). Additionally, proper optimization of the magnet width could also enhance the machine's ability to tolerate demagnetization impact, as demonstrated in (Wei and Nakamura, 2020), for an improved torque performance.

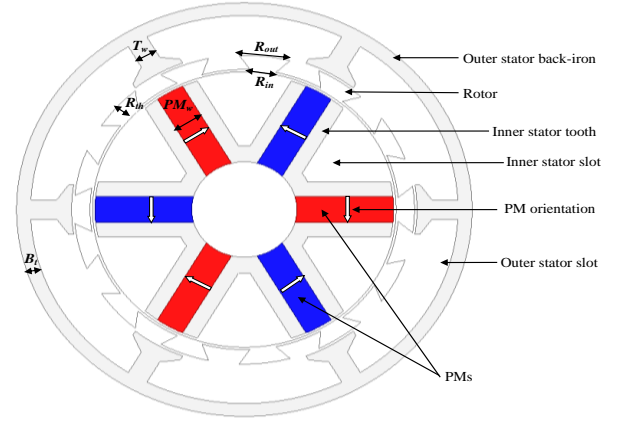
It is proved in (Zhang *et al.*, 2018) that the output torque and efficiency of a permanent magnet machine could be enhanced by modifying its structural design, especially with regard to the size and length of its permanent magnet material. (Zhang *et al.*, 2018) further revealed that the use of larger volume of magnet in a machine could result to higher output performance, though with restriction on the availability of the winding slot areas. Further, the influence of various geometric parameters on average torque of dual stator switched flux PM machine is detailed in (Evans and Zhu, 2015). It is proved that the overall electromagnetic performance of a given machine would depend on its adopted geometric parameters. Moreover, stator and rotor pole relations, electromagnetic loadings, and geometric variables are essential in the design, optimization and analysis of permanent magnet machines, due to its significant influence on the torque density (Li *et al.*, 2014).

The amount of flux around the airgap of dual stator PM machine due to the effect of tooth-tip is presented through analytical model in (Saed *et al.*, 2019), in order to predict the resultant flux-density and possibly optimize the machine accordingly for an optimum yield and for better electromagnetic performance. Again, it is important to note that analytical predictions are mainly based on series of assumptions and thus, lacks high precision most often. Nevertheless, the research in (Saed *et al.* 2019) is validated by experiments with some discrepancies from predicted analytical results, though within an acceptable tolerance of about 0.059. Moreover, the impact of design parameters on torque-speed envelope of an interior permanent magnet machine using sensorless control strategy is reported in (Kano and Matsui, 2018) with test validation. It is proved that speed range of the machine could be influenced by its geometric parameters; meanwhile, the adopted PM volume would directly affect the magnitude of induced-voltage as well as cost of the given electric machine, though, the efficiency values of such machines are comparable under different slot opening conditions. More so, it is reported in (Fan *et al.*, 2010) that a good choice of geometric parameters would not only enhance the machine's output performance, but also will reduce the attendant cost implications of not using the most optimum geometric dimension (s).

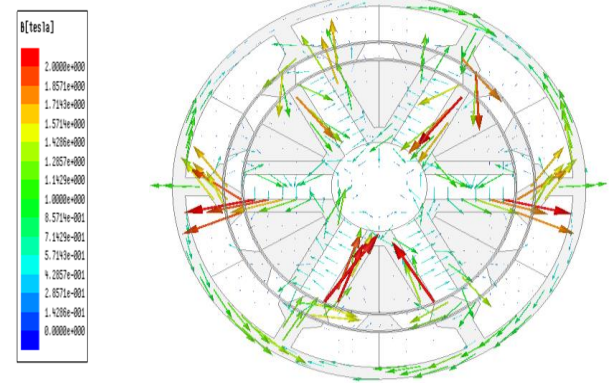
Finally, the influence of design geometric elements on induced-electromotive force and phase flux linkage of a double stator permanent magnet machine is presented in this study, with a view to determining its impact and hence, improve its overall electromagnetic output and by extension of any given electric machine by selecting the appropriate parametric value. Note that the investigated machine topology in this present study belongs to the family of flux-switching permanent magnet (FSPM) machines.

2. Methodology

The investigated machine structural diagram is given in Figure 1 (a), while its corresponding magnetic field vector on open-circuit condition is depicted in Figure 1 (b). Note that the analyzed three-phase machine has two different stators, with one section (outer part) equipped with only armature windings while the other part is furnished with both magnets and armature windings. A segmented rotor structure is sited in-between these stators. Note also that the stator and rotor parts are made of steel material while the permanent magnet material is of neodymium-iron-boron. Active length of the investigated machine and its total radius is 25 mm and 45 mm, respectively. The machine has an air gap length of 0.5 mm. The simulations are performed using finite element analysis.



(a) The developed machine structure



(b) Field vector, no load

Figure 1: Investigated machine diagram and magnetic field vector.

Optimal machine dimensions for maximum average torque of the investigated machine are obtained using the inherent evolutionary algorithm of the simulation software. However, further parametric variations of the design elements are calculated in order to estimate the potential design values that would yield the largest electromotive force and flux linkage magnitudes. The phase flux linkage (ψ) and induced-electromotive force (E) of a given double stator permanent magnet machine over a specified time (t) and at rotor angular position (θ) are obtained using (1) and (2), respectively. The time derivative of the phase flux linkage would result to phase electromotive force.

$$\psi = N_{ph} B_{max} K_{fp} F_r R_{sp} \frac{\pi D_i}{P_s} L_a \quad (1)$$

$$E = \frac{d\psi}{d\theta} \times \frac{d\theta}{dt} = \frac{d\psi}{dt} \quad (2)$$

where: N_{ph} is the phase number of turns, B_{max} is the amplitude of air gap flux density on aligned pole positions, K_{fp} is the fundamental to peak flux linkage ratio, F_r is the excitation flux to full flux ratio, R_{sp} is the stator-tooth size to pole pitch ratio, P_s is the stator pole number, D_i is the stator inner diameter, L_a is the machine's active length (Li *et al.*, 2016).

Each of the design element is assigned with an arbitrary initial value in the software, though, within acceptable limits in-line with its various sizes in proportion to the overall machine size. Each particular design element is then linked to the dimensions of other sections of the machine before subjecting the entire model to intrinsic evolutionary optimization of the adopted software, while keeping the copper loss at constant value of 30 W. The rated current of the machine model is 15 A and it is operated at a motor speed of 400 rev/min. The objective is to realize the peak value of machine output at the convergence point of the numerous finite element iteration calculations.

It is worth noting that the implemented aspect ratio (A_r) is given as a fraction of active air-gap length to machine overall diameter. Similarly, the outer rotor pole arc / pitch proportion (γ_1), and inner rotor pole arc / pitch proportion (γ_2) are estimated using the expressions in (3) and (4), respectively.

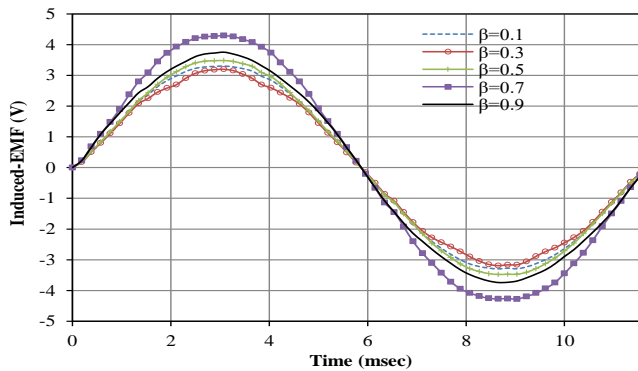
$$\gamma_1 = \frac{R_{out}}{\left(\frac{360^\circ}{P_r}\right)} \quad (3)$$

$$\gamma_2 = \frac{R_{in}}{\left(\frac{360^\circ}{P_r}\right)} \quad (4)$$

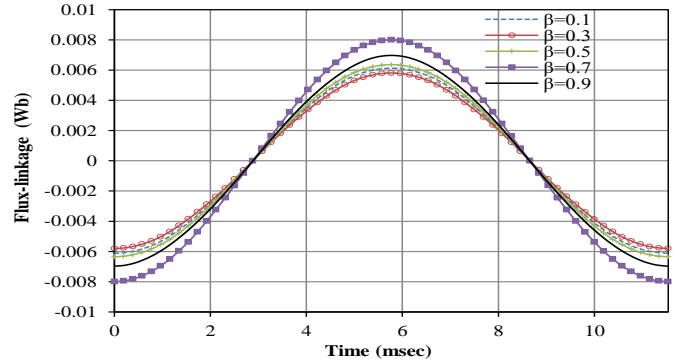
where: P_r is the number of rotor poles i.e. 13 in this present case; R_{out} and R_{in} are the respective rotor pole arcs.

3. Influence of Design Elements

Figure 2 shows the effect of conductor space opening / stator tooth pitch proportion (β) on induced-electromotive force and phase flux linkage waveforms of the analyzed machine. It is obvious that the output of these performance indices would depend on the selected value of β . It is worth noting that the largest induced-electromotive force and flux linkage output is obtained when β is 0.7, and not necessarily at the highest value of β . Note also that the obtained waveforms under this condition are basically symmetrical and sinusoidal over the complete electrical revolution, except for the situation when β is 0.3, which is relatively sinusoidal.



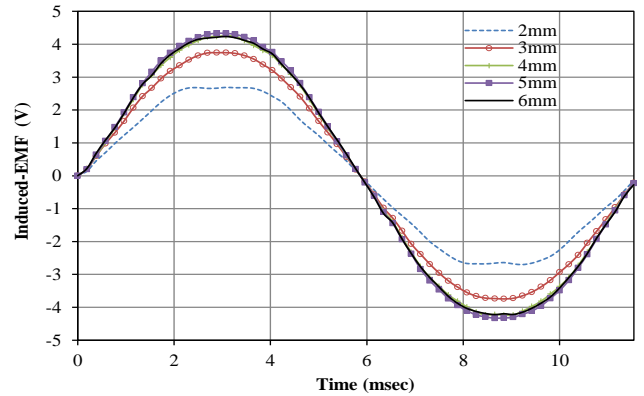
(a) Induced electromotive force versus electric period



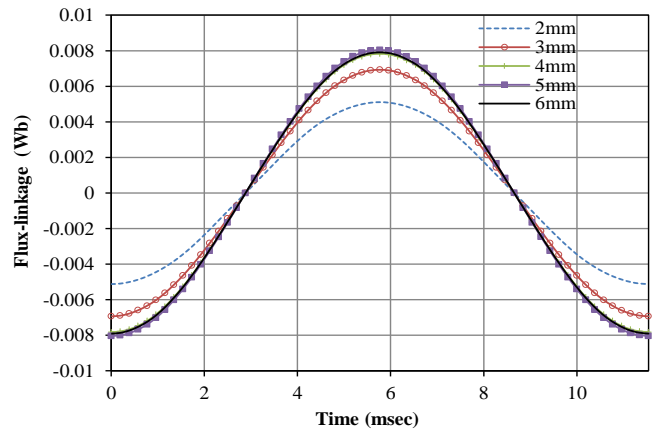
(b) Flux linkage versus electric period

Figure 2: Effect of conductor space opening/stator tooth pitch proportion on EMF and flux linkage.

Variation of the permanent magnet thickness (PM_w) with induced-electromotive force and phase flux linkage is shown Figure 3. Note that the induced-electromotive force waveform could be trapezoidal as observed at the point when the PM thickness is 2 mm; however, the largest output performance is obtained at the value of 5 mm. Therefore, it can be concluded that the resulting waveform/shape is a function of the geometric value; and this will definitely affect the machine's compatibility with control techniques.



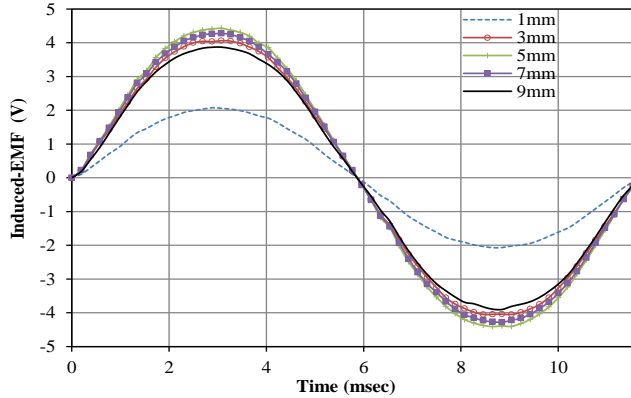
(a) Induced-electromotive force versus electric period



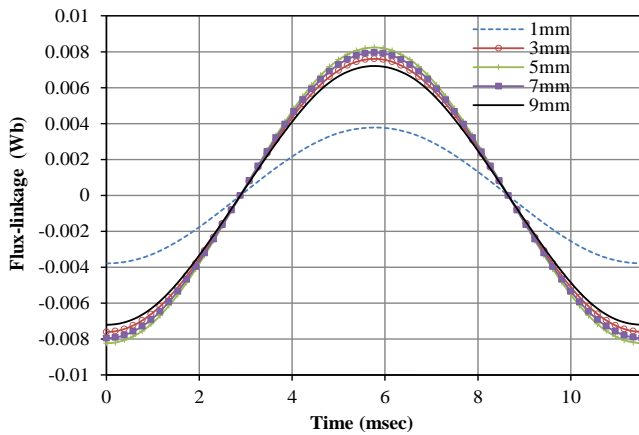
(b) Flux linkage versus electric period

Figure 3: Effect of magnet thickness on induced-electromotive force (EMF) and flux linkage.

Similarly, the impact of rotor circular width (R_{th}) on induced-electromotive force and flux linkage is depicted in Figure 4. It is worth noting that the adopted rotor circular width would invariably affect the machine's split ratio and hence, the overall electromagnetic output. The largest machine's output occurred at the rotor circular width of 5 mm and not even at the 7 mm or 9 mm point; possibly due to the indirect adverse impact of these high values on the conductor slot spaces as well as its negative impact on the resulting aspect ratio on that condition.



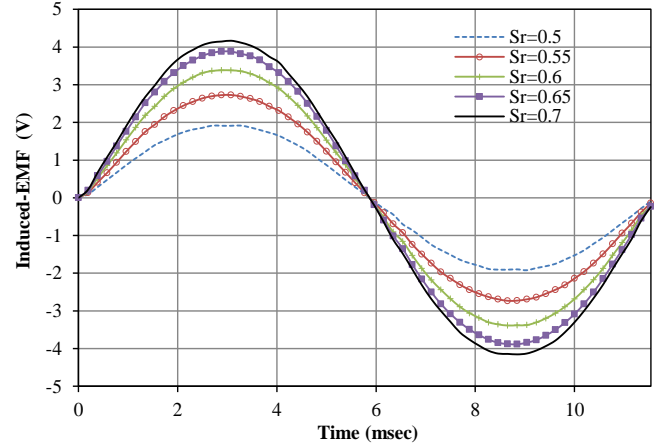
(a) Induced-electromotive force versus electric period



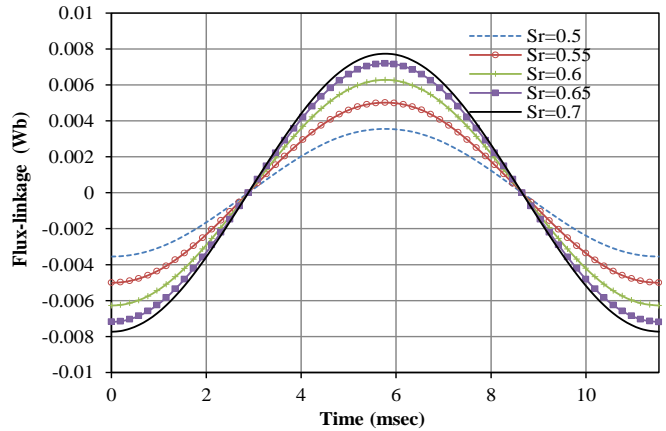
(b) Flux linkage versus electric period

Figure 4: Effect of rotor circular width on induced-electromotive force (EMF) and flux linkage.

More so, the variation of aspect ratio (A_r) with induced-electromotive and phase flux linkage is displayed in Figure 5. The highest induced-electromotive and phase flux linkage magnitude is obtained at an aspect ratio value of 0.7.



(a) Induced-electromotive force versus electric period

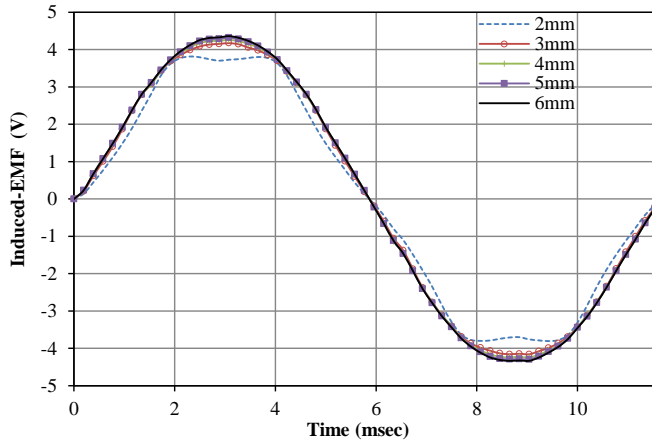


(b) Flux linkage versus electric period

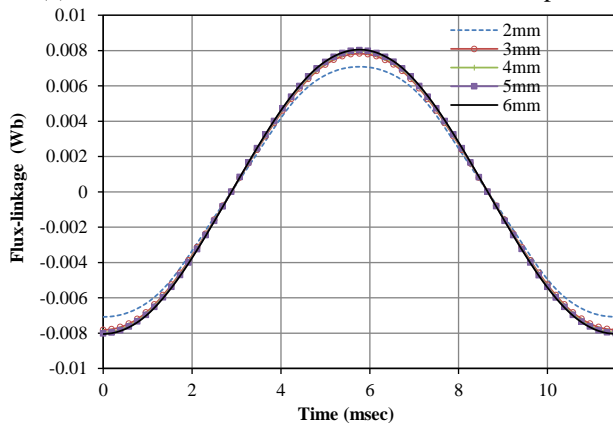
Figure 5: Effect of aspect ratio on induced-electromotive force (EMF) and flux linkage.

The completely sinusoidal nature of the waveforms in Figure 5 indicates that at such operating A_r values, there would be less voltage harmonic effects and hence, high tendency for improved electromagnetic performance, as well as increased propensity for electric machine control amenability. It is important to note that aspect ratio plays a very vital role in determining the overall performance of any electrical machine, as reported in (Zhu and Chen, 2010); Acquaviva 2018).

Figure 6 shows the effect of stator tooth-width (T_w) on induced-electromotive force and phase flux linkage waveforms. It is observed that the impact of this design element is not very strong, since the output difference amongst the varied tooth width values is insignificant. It is worth mentioning that the optimum stator tooth width of the investigated machine is 6 mm. Moreover, the deviation from the sinusoidal outline at 2 mm implies that there could be substantial amount of harmonics on the machine, at such operating point.



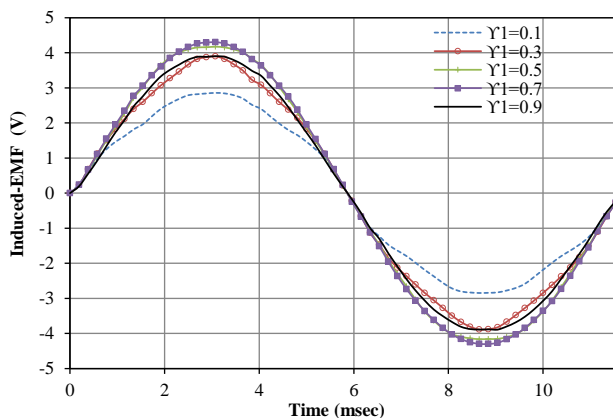
(a) Induced-electromotive force versus electric period



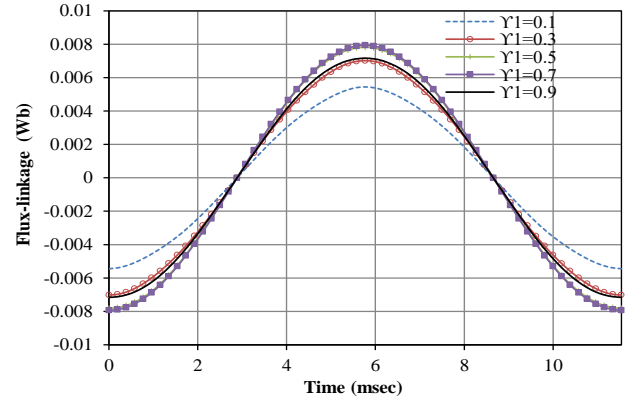
(b) Flux linkage versus electric period

Figure 6: Effect of stator tooth width on induced-electromotive force (EMF) and flux linkage.

The effect of the outer rotor pole arc / pitch proportion (γ_1) and inner rotor pole arc / pitch proportion (γ_2), on induced-electromotive force and flux linkage is displayed in Figure 7 and 8, respectively. It is shown that there is little distortions at $\gamma_1=0.1$ and $\gamma_2=0.9$, respectively. These distortions would negatively affect the overall machine performance, because it would introduce some voltage harmonics in the system.



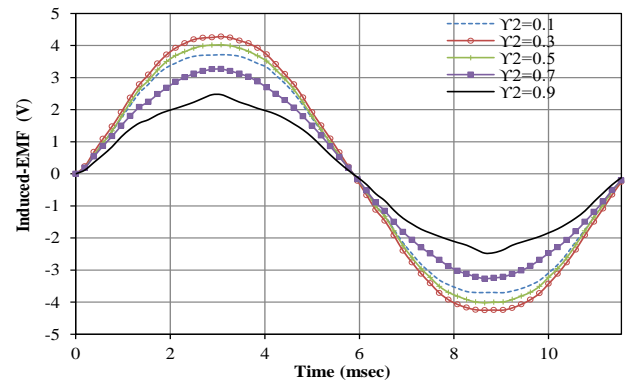
(a) Induced-electromotive force versus electric period



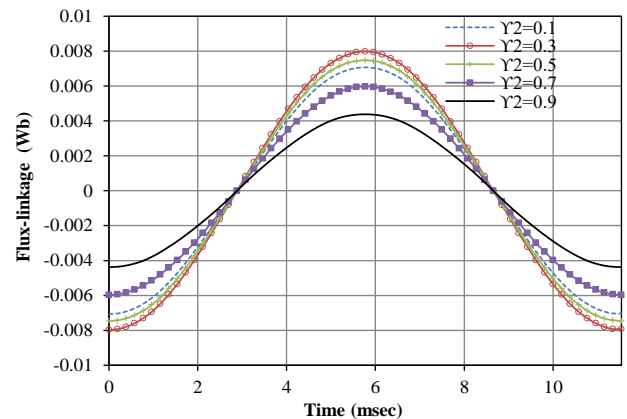
(b) Flux linkage versus electric period

Figure 7: Effect of outer rotor pole arc / pitch proportion on induced-EMF and flux linkage.

Meanwhile, the highest value of electromotive force and flux linkage is obtained when $\gamma_1=0.7$ and $\gamma_2=0.3$. It is worth stating that the resulting performances by these two design elements would be dependent on the rate of linking fluxes at the airgap region for each specific γ_1 and γ_2 instance. The resulting γ_1 value is in agreement with the obtained pole arc proportion in Wei and Nakamura (2020), though, both machines are of different structural plan.



(a) Induced-electromotive force versus electric period



(b) Flux linkage versus electric period

Figure 8: Effect of inner rotor pole arc / pitch proportion on induced-EMF and flux linkage.

Above all, it is worth noting that each of the investigated design element would influence the effectiveness of the other design elements; thus, a compromise is always needed to be reached amongst the design elements for an optimum yield to ensue. It is also worth remarking that in all cases, the phase flux linkage waveforms are consistently sinusoidal and symmetrical over the given electric period, and these are good machine attributes.

4. Conclusion

The influence of leading design elements on induced electromotive force and phase flux linkage of double stator permanent magnet machine is reported in this study, using finite element analysis approach. It can be concluded that geometric elements would invariably affect the output performance of any given electric machine; thus, good choice of optimum geometric values is critical in the design and optimization of such machines, in order to yield the best output performance and as well avoid the consequent cost effects of applying less suitable geometric values. Moreover, the influence of one particular design element would affect the output of the others, owing to its direct inter-dependence on the machine's electromagnetic reactions on both open-circuit and load conditions; and this usually gives rise to compromise amongst the chosen geometric values of the design elements. Optimum values of the design elements are: 0.7, 5 mm, 5 mm, 0.7, 6 mm, 0.7 and 0.3 for the conductor space / rotor pitch proportion, permanent magnet width, rotor circular width, aspect ratio, stator tooth-width, outer rotor pole arcs / pitch proportion and inner rotor pole arcs / pitch proportion, respectively. Meanwhile, efficient control of the investigated machine would be a direct consequence of its resulting flux linkage and induced-electromotive force waveforms; the more sinusoidal these waveforms are, the better its control proficiency. The investigated machine could be applied in low speed direct-drive applications.

References

- Acquaviva, A. (2018). Analytical electromagnetic sizing of inner rotor brushless PM machines based on split ratio optimization. *International Conference on Electrical Machines (ICEM)*, Alexandroupoli, Greece, pp. 576–582, IEEE.
- Lekic, D., and Vukosavic, S. (2020). Computationally efficient steady-state finite element simulation of multiphase PM AC machines. *IET Electric Power Applications*, Vol. 14, No. 7: 1228–1237.
- Evans, D.J., and Zhu, Z.Q. (2015). Novel partitioned stator switched flux permanent magnet machines. *IEEE Transactions on Magnetics*, Vol. 51, No. 1: 1–14.
- Fan, Y., Jiang, H., Cheng, M., and Wang, Y. (2010). An improved magnetic-gear permanent magnet in-wheel motor for electric vehicles. *IEEE Vehicle Power and Propulsion Conference*, Lille, France, pp. 1–5, IEEE.
- Kano, Y., and Matsui, N. (2018). Rotor geometry design of saliency-based sensorless controlled distributed-winding IPMSM for hybrid electric vehicles. *IEEE Transactions on Industry Applications*, Vol. 54, No. 3: pp. 2336–2348.
- Li, D., Qu, R., and Xu, W. (2014). Design process of dual-stator, spoke-array vernier permanent magnet machines. *Energy Conversion Congress and Exposition (ECCE)*, Pittsburgh, USA, pp. 2350–2357, IEEE.
- Li, D., Qu, R., Zhang, X., and Liu, Y. (2012). Optimal split ratio in switched flux permanent magnet machines. *Energy Conversion Congress and Exposition (ECCE)*, Raleigh, USA, pp. 1925–1930, IEEE.
- Li, X., Chau, K.T., Cheng, M., Hua, W., and Du, Y. (2011). An improved coaxial magnetic gear using flux focusing. *International Conference on Electrical Machines and Systems (ICEMS)*, Beijing, China, pp. 1–4, IEEE.
- Li, Y., Bobba, D., and Sarlioglu, B. (2016). A novel 6/4 flux-switching permanent magnet machine designed for high-speed operations. *IEEE Transactions on Magnetics*, Vol. 52, No. 8: 1–9.
- Saed, N., Asgari, S., and Mirasalim, M. (2019). Analysis and modeling of tooth-tip leakage fluxes in a radial-flux dual-stator machine with diametrically magnetized cylindrical permanent magnets. *CES Transactions on Electrical Machines and Systems*, Vol. 3, No. 4: pp. 382–388.
- Thomas, A.S., Zhu, Z.Q., Owen, R.L., Jewell, G.W., and Howe, D. (2009). Multiphase flux-switching permanent-magnet brushless machine for aerospace application. *IEEE Transactions on Industry Applications*, Vol. 45, No. 6: pp. 1971–1981.
- Wei, L., and Nakamura, T. (2020). Design and optimization of a partitioned stator flux-modulated memory machine. *IEEE Transactions on Magnetics*, Vol. 56, No. 4: 1–5.
- Zhang, L., Wu, L.J., Huang, X., and Fang, Y. (2018). A novel structure of doubly salient permanent magnet machine. *International Conference on Electrical Machines (ICEM)*, Alexandroupoli, Greece, pp. 2009–2015, IEEE.
- Zhang, Y., Huang, Y., Yuan, Y., Luo, J., and Chen, X. (2017). Design and analysis of a bearingless permanent-magnet machine with improved torque density for stirred tank bioreactor. *Progress in Electromagnetics Research M*, Vol. 57: pp. 151–162.
- Zhu, Z.Q., and Chen, J.T. (2010). Advanced flux-switching permanent magnet brushless machines. *IEEE Transactions on Magnetics*, Vol. 46, No. 6: pp. 1447–1453.